ACS OMEGA

http://pubs.acs.org/journal/acsodf

Article

Effects of Surface Heterogeneity of α-Quartz and α-Cristobalite on Adsorption of Crystal Violet

Cuihua Tang* and Huan Dong

Cite This: *ACS Omega* 2021, 6, 12105−12113

Read Online

ACCESS | Metrics & More | Article Recommendations

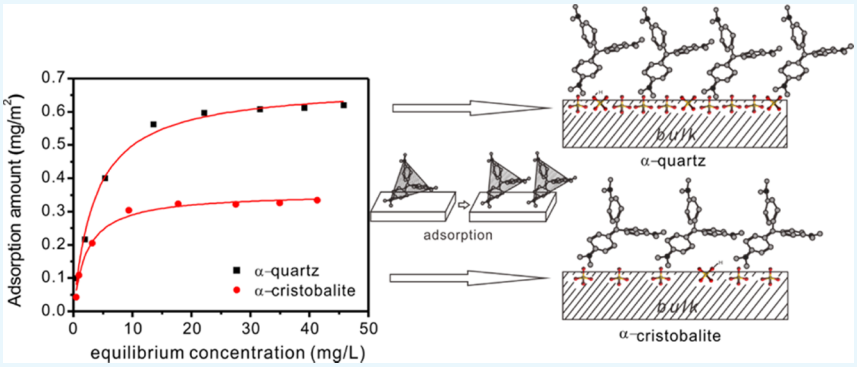

ABSTRACT: Silica minerals are a kind of important minerals and widespread on the earth's surface. They play an irreplaceable role in the whole geochemistry and environment processes. The diversity in the crystal structure of SiO_2 polymorphs might lead to the heterogeneity in their surface microstructures and properties. As two common SiO_2 polymorph minerals in soil and sediments, α-quartz and α-cristobalite have been studied for the effects of their surface heterogeneity on adsorption behaviors toward crystal violet (CV) by batch adsorption experiments in different specific surface areas (SSAs) and at different pH values and temperatures, as well as by X-ray photoelectron spectroscopy (XPS) investigation. Owing to the larger surface site density, the saturated adsorption amount of α-quartz was larger than that of α-cristobalite. It was also indicated by the larger slope of adsorption lines as a function of SSA. The adsorption capacity of both increased with increasing pH and temperature. In the thermodynamic study, the negative ΔG indicated that the adsorption of CV on the surface was spontaneous and the positive ΔH suggested that the reaction was endothermic. The well-fitted Langmuir adsorption isotherms suggested that the CV adsorption was monolayer adsorption. The adsorption interaction force was mainly involved in electrostatic attraction force between the negatively charged surface reactive sites and positively charged N atoms in the dimethylamino groups of CV. The XPS spectra of N 1s showed that the stoichiometric ratio of N_{low}/N_{high} changed from lower than 2:1 to about 2:1 as the adsorption changed from the unsaturated to saturated state. The change reflected that the spatial arrangement of adsorbed CV monomer on the mineral surface could be readjusted by lifting the average tilt angle between the average plane of the CV monomer and the sample surface during the adsorption process. Surface heterogeneity of α-quartz and α-cristobalite controlled the different distributions and postures of adsorbed CV monomers on the surface. The CV monomers adsorbed on α-quartz presented a larger average tilt angle because of its larger surface reactive site density, while α-cristobalite did conversely.

1. INTRODUCTION

Silica minerals are abundant in the earth's crust and very important to production and life. On the one hand, silica species have been extensively used in some industries, including catalysis products, electronic devices, optical instruments, and solar cells because of their unique properties.[1−3] On the other hand, as a group of significant minerals in soil and sediments, silica minerals exert unique effects on the interfacial reactions involving geochemical and environmental domains.[4−7] Adsorption of contaminants at the silica−solution interface is a vital part of the self-purification process of soil and sediments. Dye substances are well known to be widely used in many industries, such as textile, leather, dye, printing, food, and plastic industries, and also a major source of colored wastewater due to their unreasonable discharge.[8] Indiscriminate discharge of the dye wastewater not only leads to the

Received: February 13, 2021
Accepted: April 16, 2021
Published: April 26, 2021

https://doi.org/10.1021/acsomega.1c00686
ACS Omega 2021, 6, 12105−12113

pollution of soil and water but also seriously threatens the health of human beings eventually.[9] Therefore, as common minerals in the soil and sediments, silica minerals play an irreplaceable role in the migration and gathering of these dye pollutants.

Silica minerals are made up of three-dimensional arrays of linked silicon−oxygen tetrahedrons (SiO_4). The diversity of polymerization of SiO_4 tetrahedrons results in various species of silica minerals, i.e., SiO_2 polymorphs.[10] A few common crystalline SiO_2 polymorphs, including quartz, cristobalite, tridymite, etc., exist in soil and sediments. For example, α-quartz is a kind of widespread polymorph in the continental crust and α-cristobalite is mainly constituted of dustfalls of the ceramic industry and commonly distribute in soil and sediments.[11] According to the previous research works,[10,12,13] the diverse polymerization style and different crystalline structures of silica minerals may lead to the difference in surface microstructures and properties. The structure and property characteristics of surface reaction functional groups affect the interfacial physical−chemical processes to a great extent.[14] Therefore, the surface heterogeneity of SiO_2 polymorphs may affect the reaction performance at the mineral−environment interface.

Surface silanols are the major surface functional groups of silica minerals and predominantly control the interfacial reactions. A number of studies on the surface microstructures and properties of silica minerals have been carried out in the past decades. According to Legrand et al.'s research, the distribution of silicon functionality on the surface of amorphous silica was studied by ^{29}Si solid-state nuclear magnetic resonance (NMR) spectroscopy, and the evolution of single versus germinal silanols was interpreted as a result of the equilibrium of the functional groups.[11] Peng et al. further verified various kinds of silanols on the diatomite surface, such as isolated, vicinal, and germinal, interacting via H-bonds with the help of the ^1H magic-angle spinning nuclear magnetic resonance (^1H MAS NMR) technique.[15] Further, Bolis et al. demonstrated the surface heterogeneity of some SiO_2 polymorphs by determining the adsorption enthalpy and hydrophilicity/hydrophobicity using some small probe molecules such as water and alcohols.[16−18] With the wide application of molecular simulation techniques, it also has been reported that surface microstructures of some SiO_2 polymorphs were not identical,[19,20] especially on different crystal surfaces.[21,22] The species and distribution of surface silanols are bound up with the surface reactivity of SiO_2 polymorphs, and this may lead to these polymorphs showing different surface reactivities with diverse environmental contaminants.

Despite a few reported studies on the heterogeneity of SiO_2 polymorphs, this study was mainly focused on the interactions involved in SiO_2 polymorphs and some small molecules in a relatively simple environment. However, the interactions between mineral surface and various solution environment−relevant substances (especially some organic pollutants and heavy metals) determined the fate of these pollutants and exerted great effects on the surface environments of the earth. Nevertheless, limited experimental studies on the effects of surface heterogeneity of a few SiO_2 polymorphs dealing with typical organic pollutants have been reported so far, let alone reasonable reaction mechanisms cover the reaction difference. Moreover, with the development of modern technologies of surface analysis, for example, X-ray photoelectron spectroscopy (XPS), the surface reaction mechanism would be further revealed. XPS has been testified to be a feasible technique to investigate the surface chemical composition and state of minerals.[23−27] Hence, it would also be an efficient tool to detect the effects of surface heterogeneity of SiO_2 polymorphs on adsorption behavior toward contaminants at the atomic level.

To further probe the effect of surface heterogeneity of SiO_2 polymorphs on removal of organic contaminants from water, the adsorption behaviors of α-quartz and α-cristobalite toward typical cationic dye crystal violet (CV) were investigated by batch adsorption experiments. Effects of some factors, such as SSA, pH, and temperature, on adsorption were discussed in the adsorption experiments. The difference in adsorption characteristics between the two minerals was detailedly discussed, including adsorption capacity and thermodynamic parameter analysis. The XPS characterization of α-quartz and α-cristobalite before and after adsorption of CV was used to interpret the reaction mechanism. With the combination of adsorption results and XPS analyses, a schematic model of the CV dye monomer adsorbed on the surface of α-quartz and α-cristobalite was further put forward.

2. EXPERIMENTAL SECTION

2.1. Experimental Materials. The sample of α-quartz was naturally collected from Guiding, Guizhou Province of China, and the α-cristobalite sample was purchased from Veston Silicon Co., Ltd. in Guiping County, Guangxi Province of China. To acquire a relatively uniform average particle size, both samples were ground with a planetary ball mill (FRITSCH Pulverisette 6, Germany) for about 2 h. All of the powders were immersed in 0.01 M HCl solution for 24 h and then rinsed with deionized water until they were free from chloride ions. After drying, the samples were calcined in a muffle furnace at 450 °C for 12 h. The specific surface area of samples was determined by a Micromeritics ASAP 2020M specific surface area and porosity analyzer. To compare well the surface property of α-quartz and α-cristobalite, the adsorption capacity was all normalized to the specific surface area of samples.

Reagent-grade crystal violet (CV) ($C_{25}H_{30}N_3Cl{\cdot}3H_2O$, purity ≥ 99.0%), from Tianjin Kemiou Chemical Reagent Co., Ltd., was used to prepare all solutions for the adsorption experiments. All solutions were prepared in deionized water, and the solution pH was adjusted with standard acid (0.1 M HCl) and standard base (0.1 M NaOH) solutions.

2.2. Characterization Techniques. XPS characterizations were conducted on a Thermo Scientific Escalab 250 instrument equipped with an Al Kα source (10 mA, 14 kV), operating at 1486.8 eV during the measurements. The base pressure in the spectrometer analyzer chamber was lower than 2×10^{-9} mbar. The charge neutralizer filament was opened during all experiments to keep charging of the samples. To keep samples fresh and clean in the experiment, all dried mineral samples were taken to characterize as quickly as possible. The Carbon C 1s peak at 284.8 eV was used as a reference to correct the charging effect. All XPS data were analyzed by a nonlinear least-squares fit routine with Gaussian/Lorentian area band shape. The Smart background correction model was used for background correction for all spectra.

2.3. Adsorption Experiments. *2.3.1. Adsorption with Different Specific Surface Areas (SSAs).* The adsorption experiments were carried out at an ambient temperature and

https://doi.org/10.1021/acsomega.1c00686
ACS Omega 2021, 6, 12105−12113

pH 7. α-Quartz and α-cristobalite (0.4 g) with different SSAs were added to each 50 mL polypropylene centrifuge tube, and then, 20 mL of 30 mg/L CV solution was injected into each one. The solid−liquid mixtures were shaken in an incubator shaker at 160 rpm for 24 h.

2.3.2. Adsorption at Different pH Levels. The effect of pH on adsorption behavior was discussed by determining the adsorption isotherms at pH levels 4, 7, and 9. In batch adsorption experiments, 0.4 g of α-quartz and α-cristobalite powder was added into each 50 mL polypropylene centrifuge tube and then 20 mL of CV solutions with designated concentrations (5, 10, 20, 30, 40, 50, 60, 70 mg/L) were injected into each one, respectively. The pH of all suspensions was adjusted to 4. Then, the centrifuge tubes were put in an incubator shaker and shaken continuously at 160 rpm for 24 h. The experimental processes at pH 7 and 9 were the same as those at pH 4.

2.3.3. Adsorption at Different Temperatures. In consideration of the effect of temperature, the pH was kept at approximately 7, while the temperatures were set at 288, 298, and 303 K. The residual experimental process was the same as that in Section 2.3.2.

In all of the above experiments, the mixtures were centrifuged at 4200 rpm for 10 min after adsorption reactions. The supernatant solutions were carefully sampled and diluted to appropriate concentrations with deionized water. Then they were determined with an ultraviolet−visible (UV−vis) spectrophotometer (PerkinElmer Lambda 850 UV/Vis Spectrometer) at a wavelength of 583 nm. All solutions were determined in duplicate, and the average value was adopted for calculations. Blank experiments indicated no detectable CV adsorbed on the surface of centrifuge tubes. The solid samples reacted at pH 7 and 25 °C were dried in a vacuum freezing dryer for 24 h after rinsing with deionized water. The dried samples were kept in a drying apparatus, and the XPS test was conducted as soon as possible.

3. RESULTS AND DISCUSSION

3.1. Effect of Different SSAs. As for framework structural silicon-containing minerals, surface silanols are the dominantly reactive functional groups, α-quartz and α-cristobalite included.[11,28] Therefore, the reaction intensity in mineral−water interfacial reactions is closely related to their SSAs. As shown in Figure 1, there was a linear positive correlation between the adsorption amounts of CV and the SSA of α-quartz and α-cristobalite. The relation could be well suggested by two straight lines with different slopes. It is manifested that the surface reactivity of α-quartz and α-cristobalite was not completely related to their SSA, but also the surface heterogeneity of reactivity was rooted in surface microstructures and properties. The slope value of α-quartz was a little larger than that of α-cristobalite, which indicated that the adsorption capacity of α-quartz was larger. To compare better the surface difference between the two minerals, the adsorption amounts of CV were normalized to both their unit surface areas in the batch adsorption experiments.

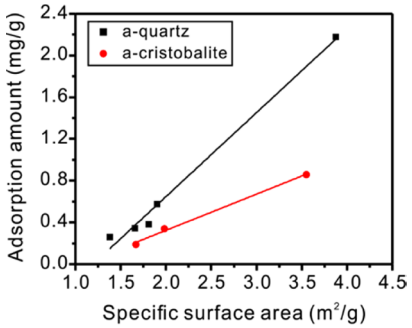

Figure 1. Amount of adsorbed CV as a function of SSAs of α-quartz and α-cristobalite.

3.2. Effect of pH. Adsorption isotherms can illustrate well the adsorption characteristics between minerals and contaminants. The pH of the solution is a significant effect factor in the adsorption behavior of minerals. Therefore, the effect of pH on CV adsorption on α-quartz and α-cristobalite was discussed by determined adsorption isotherms at pH 4, 7, and 9. According to adsorption isotherms in Figure 2, the adsorption capacity of the two silica minerals toward CV increased with increasing solution pH. All of the adsorption data fitted well with the Langmuir isotherms, suggesting that CV adsorption on the surface was monolayer adsorption. Based on the fitting results, the saturated adsorption amounts of α-quartz and α-cristobalite were 0.55 and 0.21 mg/m^2 at pH 4, respectively. With the pH increasing to 7, the saturated adsorption amount also increased a little. The maxima of adsorption capacity of α-quartz and α-cristobalite were 1.19 and 0.55 mg/m^2 at pH 9, respectively. In the studied solution pH regions, CV mainly existed in the form of cations, while the surfaces of α-quartz and α-cristobalite were negatively charged because their points of zero charge (pH_{pzc}) were 2.8 and 3.2, respectively.[29,30] Therefore, the negatively charged mineral surface was favorable for the adsorption of positively charged CV^+ cations. Further, the dehydration of surface silanols on α-quartz and α-cristobalite was much easier to happen in an increased pH environment.[31] Therefore, the more the negative charge on the surface, the more the CV^+ cations adsorbed on the surface. The electrostatic attraction force between CV^+ cations and the negatively charged surfaces of α-quartz and α-cristobalite was the dominant reaction force. In comparison with that of α-cristobalite, the adsorption capacity of α-quartz was larger, which was because the surface reactive site density of α-quartz was larger than that of α-cristobalite.[29,32]

3.3. Thermodynamic Analysis. The effect of temperature was also investigated at 288, 298, and 303 K. As shown in Figure 3, the adsorption amounts of CV on α-quartz and α-cristobalite increased with increasing temperature. The adsorption capacities of both α-quartz and α-cristobalite were the weakest at 288 K, 0.56 and 0.23 mg/m^2, respectively. When the reaction temperature was increased to 298 K, even to 303 K, the saturated CV adsorption amounts of α-quartz increased from 0.68 to 0.95 mg/m^2. Correspondingly, the adsorption capacity of α-cristobalite also increased from 0.36 to 0.47 mg/m^2 as the temperature increased.

The thermodynamic parameters, such as the Gibbs free energy (ΔG), enthalpy (ΔH), and entropy (ΔS), could be calculated from the experiments at different temperatures by the following equations[33]

$$\Delta G = -RT \ln K \quad (1)$$

$$\ln K = \frac{\Delta S}{R} - \frac{\Delta H}{RT} \quad (2)$$

https://doi.org/10.1021/acsomega.1c00686
ACS Omega 2021, 6, 12105−12113

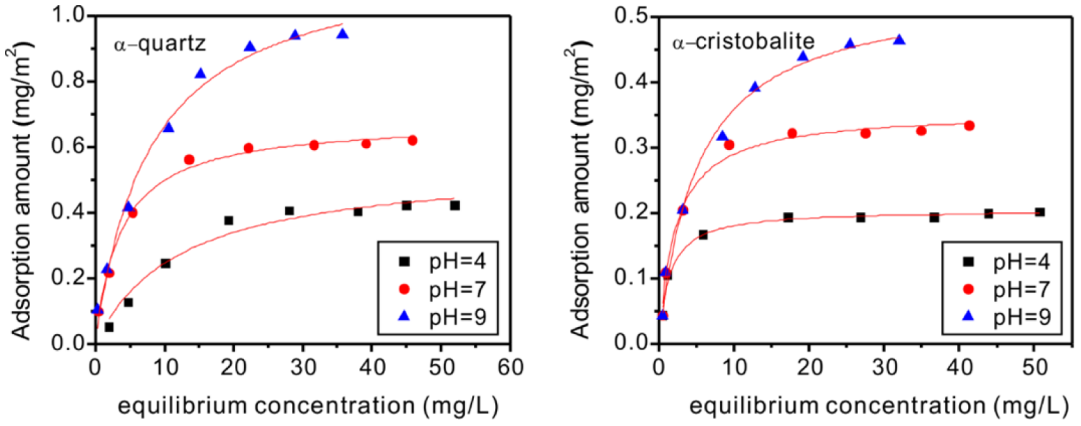

Figure 2. Adsorption isotherms of α-quartz and α-cristobalite toward CV at pH 4, 7, and 9.

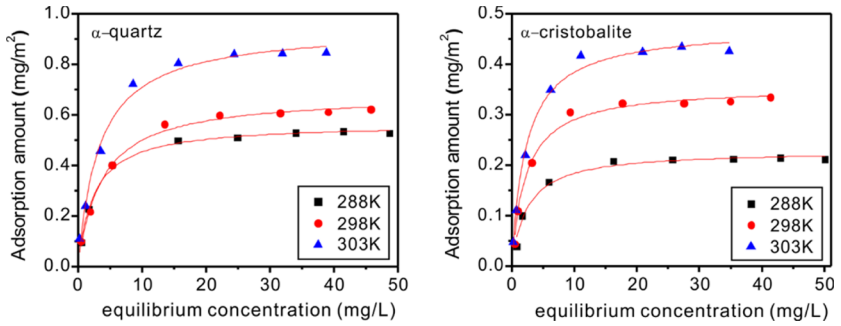

Figure 3. Adsorption isotherms of α-quartz and α-cristobalite toward CV at 288, 298, and 303 K.

where R is the gas constant (8.3145 J/(mol K)), T is the absolute temperature in kelvin (K), and K is the distribution coefficient for adsorption determined as

$$K = \frac{C_{Ae}}{C_e} \tag{3}$$

where C_e is the equilibrium concentration of CV after reaction (mg/L) and C_{Ae} is the adsorption amount of CV per liter of solution at equilibrium (mg/L). ΔH and ΔS could be calculated from the slope and intercept of the van't Hoff plots of ln K versus $1/T$ (Table 1). The negative ΔG values

Table 1. Thermodynamic Parameters for the Adsorption of CV on α-Quartz and α-Cristobalite

	ΔG (kJ/mol)				
	288 K	298 K	303 K	ΔH (kJ/mol)	ΔS (J/(mol·K))
α-quartz	−1.90	−3.11	−4.01	37.78	137.60
α-cristobalite	−0.20	−1.01	−1.29	21.02	73.75

indicated that adsorption of CV on both α-quartz and α-cristobalite was favorable and spontaneous. The positive ΔH values demonstrated that CV adsorption was an endothermic process. The larger ΔH value of α-quartz (37.78 kJ/mol) than that of α-cristobalite (21.02 kJ/mol) may imply a much different reaction behavior and spatial arrangement of CV monomers on its surface.[32] An increase in the randomness at the solid−solution interface, implied by the positive ΔS values, reflected some more possible arrangements of CV monomers.[34] This would be further discussed in the following XPS analysis parts. The different thermal effects on CV adsorption were also a good indicator of the effect of surface heterogeneities of α-quartz and α-cristobalite on the interfacial reaction behaviors.

3.4. XPS Characterization. XPS is used to investigate the interfacial reaction between minerals and adsorbates, especially for their chemical states. The XPS spectra of α-quartz and α-cristobalite with unsaturated or saturated CV adsorption at pH 7 and 298 K were investigated. The emission lines of some relevant elements, such as O, Si, and N, have been analyzed in detail. XPS spectra of the O atom and its best fit lines of samples before and after CV adsorption are shown in Figure 4. The O 1s peaks of α-quartz and α-cristobalite were both at 532.6 eV before the reaction. After CV adsorption, the enveloping broad lines of O 1s in α-quartz and α-cristobalite shifted to lower binding energy. The best fit of the negatively shifting enveloping peak could be separated into two peaks, centering at 532.6 and 531.8 eV, respectively. The negative shifts implied that the chemical environment of surface oxygen atoms changed from an electroneutral one to a more electronegative one. The relatively higher solution pH in the experiments than the pH_{pzc} of α-quartz and α-cristobalite resulted in deprotonation of surface silanols on α-quartz and α-cristobalite. So, the negative surface was favorable for the adsorption of cationic substances as follows[30]

$$>SiOH + OH^- \rightarrow >SiO^- + H_2O$$

$$>SiO^- + M^+ \rightarrow >SiO - M$$

Similar to previous studies,[27,35,36] the observed O 1s peak at about 531.8 eV was attributed to the O atoms in the structure of Si−O−M (M stood for adsorbate CV) of α-quartz and α-cristobalite. The intensity of the corresponding peak increased

https://doi.org/10.1021/acsomega.1c00686
ACS Omega 2021, 6, 12105−12113

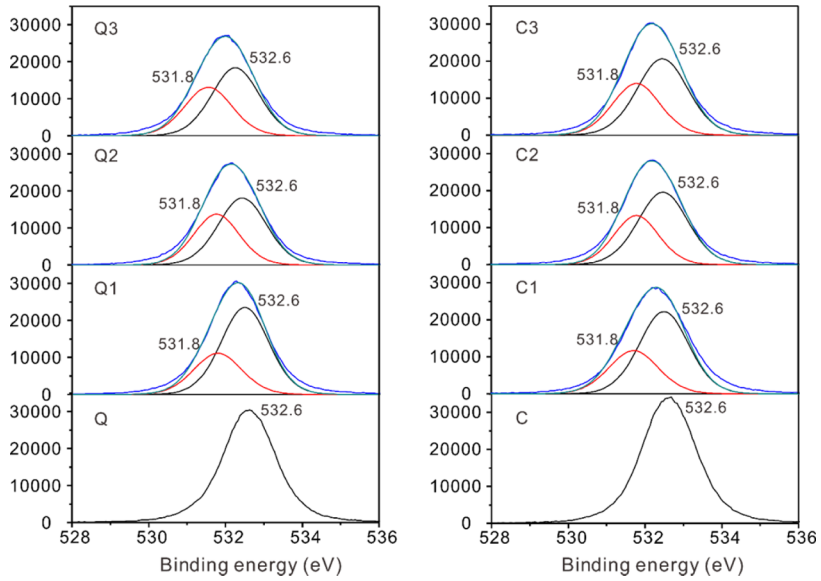

Figure 4. XPS spectra of the O 1s lines of α-quartz (Q), α-quartz with unsaturated CV adsorption (Q1 and Q2, the adsorption amount of Q2 was larger than that of Q1), α-quartz with saturated CV adsorption (Q3), α-cristobalite (C), α-cristobalite with unsaturated CV adsorption (C1 and C2, the adsorption amount of C2 was larger than that of C1), and α-cristobalite with saturated CV adsorption (C3).

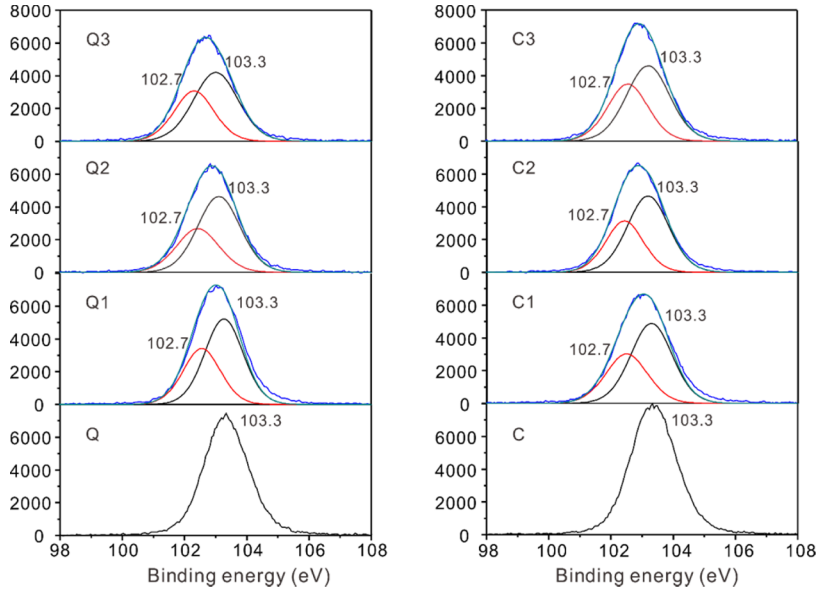

Figure 5. XPS spectra of the Si 2p lines of α-quartz (Q), α-quartz with unsaturated CV adsorption (Q1 and Q2, the adsorption amount of Q2 was larger than that of Q1), α-quartz with saturated CV adsorption (Q3), α-cristobalite (C), α-cristobalite with unsaturated CV adsorption (C1 and C2, the adsorption amount of C2 was larger than that of C1), and α-cristobalite with saturated CV adsorption (C3).

with increasing adsorbed CV amounts and reached a maximum as the adsorption reached to a saturation state.

The XPS spectra of Si 2p also provided valuable information on the adsorption characteristics of α-quartz and α-cristobalite. The Si 2p peak of α-quartz and α-cristobalite before the reaction was at 103.3 eV. The binding energies of Si 2p peaks of α-quartz and α-cristobalite loading different CV amounts showed a negative shift compared with that without CV loading. (Figure 5). It resembled the change of O 1s lines of that CV adsorption and nonadsorption. The enveloping peak could be divided into two different peaks at 103.3 and 102.7 eV. The negative shift was ascribed to the peak with a lower binding energy of 102.7 eV because of the interaction with silicon atoms as CV^+ cations adsorbed on the surfaces of α-quartz and α-cristobalite.

CV dye is a sort of typical cationic dye, and the schematic model is depicted in Figure 6. The structure of the CV molecule is similar to that of methylene blue, a cationic dye with a near-planar structure. The CV molecule contains three *N* atoms, but the three methylene groups form an angle of 30° with the sp^2 orbital of the middle carbon atom, so the entire molecular structure is propeller-shaped.[37] The positive charge in the structure is equally stabilized in the whole molecule because of π^* resonance.[38] Once the π^* resonance is interfered with by interaction, the positive charge will be reallocated unequally on the nitrogen atoms of the dimethylamino groups in the structure.

https://doi.org/10.1021/acsomega.1c00686
ACS Omega 2021, 6, 12105−12113

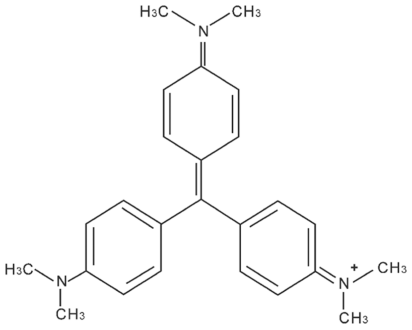

Figure 6. Schematic model of the CV cation.

The binding energy of N 1s showed significant differences between N atoms in pure CV and that adsorbed on the mineral surface. The N 1s emission line in pure CV showed a narrow and symmetric peak at 399.2 eV with a full width at half-maximum (FWHM) of 1.3 eV, indicating an identical chemical environment for all N atoms.[23] Upon adsorption, the single peak was divided into two different peaks with binding energies at 399.2 eV (N_{low}) and 401.2 eV (N_{high}), respectively, which was clearly depicted in the best fit of N regions (Figure 7). The division of the single peak could be attributed to restabilization of the positive charge at one of the dimethylamino groups in the CV adsorbed on the surface, resulting in two species of N atoms in different atomic environments. The detailed information about the N 1s peak (e.g., binding energy, FWHM, and distribution) was listed in Table 2. The stoichiometric ratio of the two N atoms (N_{low}/N_{high}) increased to about 2:1 with the CV adsorption reaching saturation. It implied that the geometric arrangement of adsorbed CV monomers was readjusted with an increase in the adsorption amounts. The stabilization of CV monomers on the mineral surface was a compromise among kinds of surface reaction forces, including electrostatic attraction force, electrostatic repulsion force of neighboring monomers, van der Waals force, and so on. First, the negatively charged surface sites interacted with the positively charged N of CV cations by electrostatic force. If the surface space of α-quartz and α-cristobalite was large enough to accommodate adsorbed CV monomers, the monomers preferentially tended to locate on the surface with a larger average contact area. This means that the other end of the adsorbed CV would interact with the redundant electronegative surface sites. However, the electrostatic interaction was much weaker because the positive charge was mainly focused on one nitrogen atom of the dimethylamino group. When another CV^+ cation got close to the surface to be adsorbed, this weaker interactive force would be broken up by the stronger electrostatic attraction force between surface reactive sites and the nitrogen atom with a positive charge in the CV^+ cation. Hence, the orientation of the adsorbed CV monomers would be readjusted. The readjustment of the arrangement of adsorbed CV monomers on the surface would result in the average tilt angle to upraise. Followingly, the temporarily unavailable surface sites sheltered by the adsorbed CV monomer were exposed again and became active to adsorb CV^+ cations. Therefore, the much larger the density of surface reactive sites, the more the CV adsorbed and the much larger the average tilt angle. That is, the average tilt angle of α-quartz was larger than that of α-cristobalite.

Table 2. Parameters of Best Fit of the N 1s XPS Spectra for Pure CV and α-Quartz and α-Cristobalite with Adsorbed CV

	binding energy (eV)	FWHM (eV)	distribution (%)	ratio of N_{low}/N_{high}
CV	399.2	1.3	100	
Q1	399.2	1.4	55.0	1.22:1
	401.2	1.7	45.0	
Q2	399.2	1.4	66.7	2.00:1
	401.2	1.8	33.3	
Q3	399.2	1.4	67.8	2.11:1
	401.2	1.8	32.2	
C1	399.2	1.5	59.0	1.44:1
	401.2	1.8	41.0	
C2	399.2	1.4	64.9	1.85:1
	401.2	1.7	35.1	
C3	399.2	1.6	66.3	1.97:1
	401.2	1.7	33.7	

3.5. Adsorption Model. The adsorption schematic diagrams of α-quartz and α-cristobalite toward CV and the different behaviors resulting from surface differences in

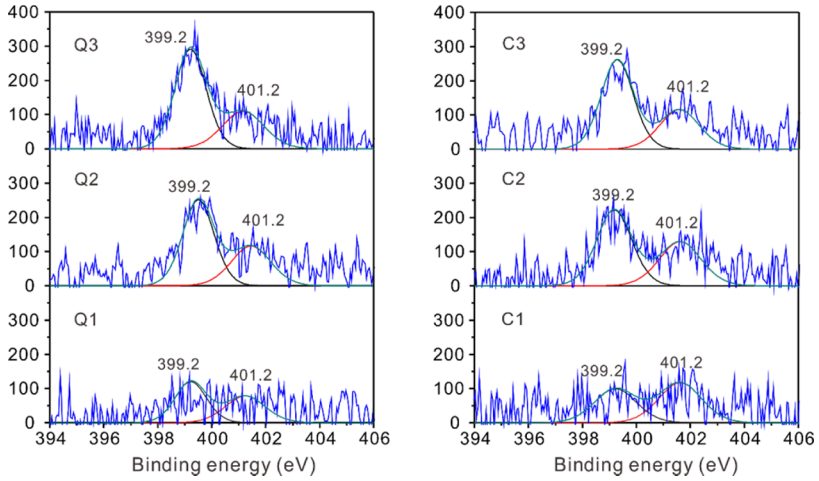

Figure 7. XPS spectra of the N 1s lines of α-quartz with unsaturated CV adsorption (Q1 and Q2, the adsorption amount of Q2 was larger than that of Q1), α-quartz with saturated CV adsorption (Q3), α-cristobalite with unsaturated CV adsorption (C1 and C2, the adsorption amount of C2 was larger than that of C1), and α-cristobalite with saturated CV adsorption (C3).

https://doi.org/10.1021/acsomega.1c00686
ACS Omega 2021, 6, 12105−12113

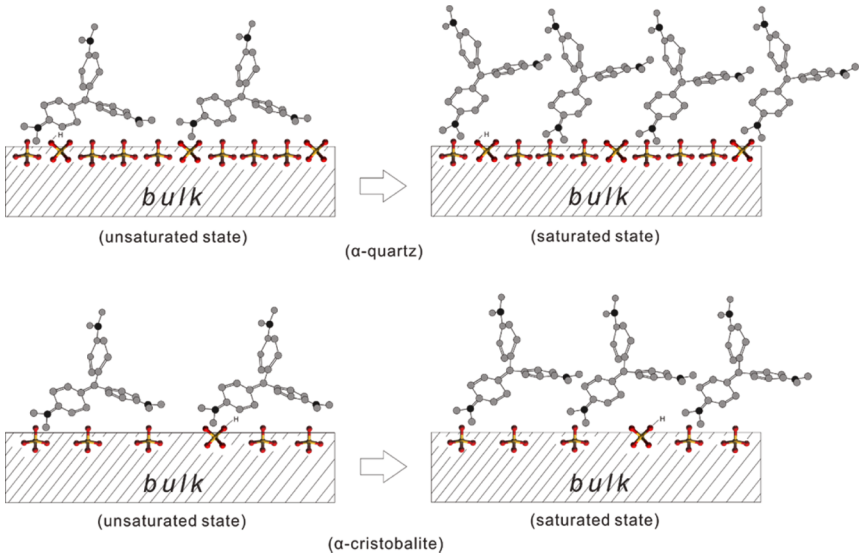

Figure 8. Schematic diagram of the adsorption process of α-quartz and α-cristobalite toward CV.

structures and properties are depicted in Figure 8. The diagram clearly demonstrated the changes in the geometric arrangement of adsorbed CV monomers on α-quartz and α-cristobalite from the unsaturated to saturated state during the adsorption process. The positively charged CV^+ cations were attracted toward the negatively charged surfaces of α-quartz and α-cristobalite by electrostatic attraction force. Under the unsaturated state, the CV^+ monomer with a positively charged N atom was adsorbed on the surface with a larger contact area. Therefore, the CV monomer lied on the surface at a relatively smaller tilt angle between the average plane of the CV monomer and mineral surface. Many surface sites were shielded by the flat CV monomer. With the increase of CV adsorption amount to saturation, the weak force between the sample surface and less positively charged N atoms of the CV monomer was broken by the adsorbed CV monomer. The tilt angle became large and the shielded surface sites became reavailable to adsorb CV^+ cations. The surface reactive site density of α-quartz and α-cristobalite affected the spatial arrangement of adsorbed CV monomers. When the CV monomer was adsorbed on the surface of α-quartz at the initial stage, more surface sites were shielded by the laying monomer due to its larger reactive site density, compared with that of α-cristobalite. With the increase of adsorption amount, more energy was needed to elevate the weakly interactive end of the adsorbed CV monomer, corresponding to a relatively higher ΔH value of α-quartz in thermodynamical analysis. Moreover, the larger adsorption capacity of α-quartz may lead the average tilt angle to be larger because of the orientation adjustment by the electrostatic repulsion between the adsorbed CV monomers. Thus, the effect of surface heterogeneity in microstructure and property of α-quartz and α-cristobalite on adsorption behavior included not only the different adsorption amounts but also the various arrangements of adsorbed CV monomers on the surface. Based on the research described above, a deep understanding of the role of different SiO_2 polymorphs minerals in environmental remediation and industrial application was obtained.

4. CONCLUSIONS

The main purpose of this paper was to discuss the effects of surface heterogeneity in microstructure and property of α-quartz and α-cristobalite on the adsorption behaviors toward CV. The adsorption performance was studied in batch experiments in different SSAs and at different pH levels and temperatures. XPS investigation was adopted to explore the adsorption characteristics of α-quartz and α-cristobalite toward CV. The adsorption capacity of α-quartz was a little larger, indicated by a larger slope of the adsorption line as a function of SSA. The saturated adsorption amounts of α-quartz and α-cristobalite both increased with increasing pH and temperature. In thermodynamic research, the negative ΔG values suggested that adsorption of CV on the surface was spontaneous and the positive ΔH values indicated an endothermic reaction. The interaction between α-quartz and α-cristobalite and CV cations was mainly involved in electrostatic attraction between negatively charged surface reactive sites and positively charged N atoms of the dimethylamino groups in CV cations. This was identified by the XPS spectra of O and Si atoms. The XPS spectra of N 1s showed that the stoichiometric ratio of N_{low}/N_{high} changed from lower than 2:1 to about 2:1 as the adsorption changed from the unsaturated to saturated state. The change indicated that the orientation of CV monomers adsorbed on the surface could be readjusted by lifting the average tilt angle between the average plane of the CV monomer and the sample surface during the whole adsorption process. The study further revealed the effect of surface microstructure and property of α-quartz and α-cristobalite on reactions by experimental methods. As one sort of abundant mineral in the crust, the obtained information provided a comprehensive insight into surface heterogeneity of polymorphous minerals and also was of significant importance for better understanding the role of SiO_2 polymorphs minerals in various environments.

AUTHOR INFORMATION

Corresponding Author

Cuihua Tang − *College of Resources and Environment, Yangtze University, Wuhan 430100, China; Hubei Key Laboratory of Petroleum Geochemistry and Environment,*

https://doi.org/10.1021/acsomega.1c00686
ACS Omega 2021, 6, 12105−12113

Yangtze University, Wuhan 430100, China; Key Laboratory of Exploration Technologies for Oil and Gas Resources, Yangtze University, Ministry of Education, Wuhan 430100, China; orcid.org/0000-0002-8412-8233; Email: tch880710@163.com

Author

Huan Dong − *School of Geosciences, Yangtze University, Wuhan 430100, China*

Complete contact information is available at: https://pubs.acs.org/10.1021/acsomega.1c00686

Notes

The authors declare no competing financial interest.

■ ACKNOWLEDGMENTS

This work was supported by the National Natural Science Foundation of China (Grant No. 41703108) and the National Natural Science Foundation of China (Grant No. 41802085).

■ REFERENCES

(1) Hwang, S. H.; Shin, D. H.; Yun, J.; Kim, C.; Choi, M.; Jang, J. SiO_2 /TiO_2 Hollow Nanoparticles Decorated with Ag Nanoparticles: Enhanced Visible Light Absorption and Improved Light Scattering in Dye-Sensitized Solar Cells. *Chem. - Eur. J.* **2014**, *20*, 4439−4446.

(2) Gerasimova, N. G. CaF_2, MgF_2, SiO_2, Al_2O_3, SiC, LiF, BaF_2, and ZrO_2 optical single crystals used in studies in the VUV spectral region. *Instrum. Exp. Tech.* **2006**, *49*, 408−412.

(3) Hopkinson, L.; Roberts, S.; Herrington, R.; Wilkinson, J. The nature of crystalline silica from the TAG submarine hydrothermal mound, 26 degrees N Mid Atlantic Ridge. *Contrib. Mineral. Petrol.* **1999**, *137*, 342−350.

(4) Wang, J.; Mao, B.; White, M. G.; Burda, C.; Gole, J. L. Interactive metal ion-silicon oxidation/reduction processes on fumed silica. *RSC Adv.* **2012**, *2*, 10209−10216.

(5) Bakos, T.; Rashkeev, S. N.; Pantelides, S. T. Reactions and diffusion of water and oxygen molecules in amorphous SiO_2. *Phys. Rev. Lett.* **2002**, *88*, No. 055508.

(6) Freedman, Y. E.; Magaritz, M.; Long, G. L.; Ronen, D. Interaction of metal with mineral surfaces in a natural groundwater environment. *Chem. Geol.* **1994**, *116*, 111−121.

(7) James, R. O.; Healy, T. W. Adsorption of hydrolyzable metal ions at the oxide—water interface. II. Charge reversal of SiO_2 and TiO_2 colloids by adsorbed Co(II), La(III), and Th(IV) as model systems. *J. Colloid Interface Sci.* **1972**, *40*, 53−64.

(8) Leodopoulos, C.; Doulia, D.; Gimouhopoulos, K. Adsorption of Cationic Dyes onto Bentonite. *Sep. Purif. Rev.* **2015**, *44*, 74−107.

(9) Eren, E.; Afsin, B. Investigation of a basic dye adsorption from aqueous solution onto raw and pre-treated sepiolite surfaces. *Dyes Pigm.* **2007**, *73*, 162−167.

(10) Koretsky, C. M.; Sverjensky, D. A.; Sahai, N. A model of surface site types on oxide and silicate minerals based on crystal chemistry; implications for site types and densities, multi-site adsorption, surface infrared spectroscopy, and dissolution kinetics. *Am. J. Sci.* **1998**, *298*, 349−438.

(11) Legrand, A.; Taïbi, H.; Hommel, H.; Tougne, P.; Leonardelli, S. Silicon functionality distribution on the surface of amorphous silicas by ^{29}Si solid state NMR. *J. Non-Cryst. Solids* **1993**, *155*, 122−130.

(12) Wang, P.; Pan, Z. L.; Weng, L. B. *Systermatic Mineralogy*; Geology Publisher: Beijing, 1982; pp 58−59.

(13) Kasar, S.; Kumar, S.; Kar, A. S.; Godbole, S. V.; Tomar, B. S. Sorption of Eu(III) by amorphous titania, anatase and rutile: Denticity difference in surface complexes. *Colloids Surf., A* **2013**, *434*, 72−77.

(14) Manceau, A.; Schlegel, M.; Nagy, K. L.; Charlet, L. Evidence for the formation of trioctahedral clay upon sorption of Co^{2+} on quartz. *J. Colloid Interface Sci.* **1999**, *220*, 181−197.

(15) Yuan, P.; Wu, D.; Chen, Z.; Chen, Z.; Lin, Z.; Diao, G.; Peng, J. ^{1}H MAS NMR spectra of hydroxyl species on diatomite surface. *Chin. Sci. Bull.* **2001**, *46*, 1112−1115.

(16) Bolis, V.; Cavenago, A.; Fubini, B. Surface heterogeneity on hydrophilic and hydrophobic silicas: water and alcohols as probes for H-bonding and dispersion forces. *Langmuir* **1997**, *13*, 895−902.

(17) Fubini, B.; Bolis, V.; Cavenago, A.; Garrone, E.; Ugliengo, P. Structural and induced heterogeneity at the surface of some SiO_2 polymorphs from the enthalpy of adsorption of various molecules. *Langmuir* **1993**, *9*, 2712−2720.

(18) Bolis, V.; Fubini, B.; Marchese, L.; Martra, G.; Costa, D. Hydrophilic and Hydrophobic Sites on Dehydrated Crystalline and Amorphous Silicas. *J. Chem. Soc., Faraday Trans.* **1991**, *87*, 497−505.

(19) Murashov, V.; Harper, M.; Demchuk, E. Impact of silanol surface density on the toxicity of silica aerosols measured by erythrocyte haemolysis. *J. Occup. Environ. Hyg.* **2006**, *3*, 718−723.

(20) Bourova, E.; Parker, S. C.; Richet, P. High-temperature structure and dynamics of coesite (SiO_2) from numerical simulations. *Phys. Chem. Miner.* **2004**, *31*, 569−579.

(21) Musso, F.; Sodupe, M.; Corno, M.; Ugliengo, P. H-bond features of fully hydroxylated surfaces of crystalline silica polymorphs: A periodic B3LYP study. *J. Phys. Chem. C* **2009**, *113*, 17876−17884.

(22) Murashov, V. V.; Demchuk, E. Surface sites and unrelaxed surface energies of tetrahedral silica polymorphs and silicate. *Surf. Sci.* **2005**, *595*, 6−19.

(23) Fischer, D.; Caseri, W. R.; Hähner, G. Orientation and electronic structure of ion exchanged dye molecules on mica: An X-ray absorption study. *J. Colloid Interface Sci.* **1998**, *198*, 337−346.

(24) Zhang, Q.; Wen, S.; Feng, Q.; Liu, Y. Activation mechanism of lead ions in the flotation of sulfidized azurite with xanthate as collector. *Miner. Eng.* **2021**, *163*, No. 106809.

(25) Zhang, Q.; Wen, S.; Feng, Q.; Liu, J. Surface modification of azurite with lead ions and its effects on the adsorption of sulfide ions and xanthate species. *Appl. Surf. Sci.* **2021**, *543*, No. 148795.

(26) Han, G.; Wen, S.; Wang, H.; Feng, Q. Selective adsorption mechanism of salicylic acid on pyrite surfaces and its application in flotation separation of chalcopyrite from pyrite. *Sep. Purif. Technol.* **2020**, *240*, No. 116650.

(27) Duval, Y.; Mielczarski, J. A.; Pokrovsky, O. S.; Mielczarski, E.; Ehrhardt, J. J. Evidence of the existence of three types of species at the quartz-aqueous solution interface at pH 0-10: XPS surface group quantification and surface complexation modeling. *J. Phys. Chem. B* **2002**, *106*, 2937−2945.

(28) Brady, P. V. *The Physics and Chemistry of Mineral Surfaces*; CRC Press: Florida, 1996; pp 56−58.

(29) Tang, C.; Zhu, J.; Li, Z.; Zhu, R.; Zhou, Q.; Wei, J.; He, H.; Tao, Q. Surface chemistry and reactivity of SiO_2 polymorphs: A comparative study on α-quartz and α-cristobalite. *Appl. Surf. Sci.* **2015**, *355*, 1161−1167.

(30) Pokrovsky, O. S.; Golubev, S. V.; Mielczarski, J. A. Kinetic evidences of the existence of positively charged species at the quartz-aqueous solution interface. *J. Colloid Interface Sci.* **2006**, *296*, 189−194.

(31) Zhang, J.; Cai, D. Q.; Zhang, G. L.; Cai, C. J.; Zhang, C. L.; Qiu, G. N.; Zheng, K.; Wu, Z. Y. Adsorption of methylene blue from aqueous solution onto multiporous palygorskite modified by ion beam bombardment: Effect of contact time, temperature, pH and ionic strength. *Appl. Clay Sci.* **2013**, *83-84*, 137−143.

(32) Tang, C.; Zhu, J.; Zhou, Q.; Wei, J.; Zhu, R.; He, H. Surface heterogeneity of SiO_2 polymorphs: an XPS investigation of α-quartz and α-cristobalite. *J. Phys. Chem. C* **2014**, *118*, 26249−26257.

(33) Eloussaief, M.; Jarraya, I.; Benzina, M. Adsorption of copper ions on two clays from Tunisia: pH and temperature effects. *Appl. Clay Sci.* **2009**, *46*, 409−413.

(34) Zhang, L.; Zhang, H.; Guo, W.; Tian, Y. Removal of malachite green and crystal violet cationic dyes from aqueous solution using activated sintering process red mud. *Appl. Clay Sci.* **2014**, *93*−*94*, 85−93.

(35) Weissenrieder, J.; Kaya, S.; Lu, J.-L.; Gao, H.-J.; Shaikhutdinov, S.; Freund, H.-J.; Sierka, M.; Todorova, T.; Sauer, J. Atomic structure of a thin silica film on a Mo (112) substrate: A two-dimensional network of SiO_4 tetrahedra. *Phys. Rev. Lett.* **2005**, *95*, No. 076103.
(36) Kaya, S.; Weissenrieder, J.; Stacchiola, D.; Shaikhutdinov, S.; Freund, H.-J. Formation of an ordered ice layer on a thin silica film. *J. Phys. Chem. C* **2007**, *111*, 759−764.
(37) Gomes de Mesquita, A. H.; MacGillavry, C. H.; Eriks, K. The structure of triphenylmethyl perchlorate at 85 °C. *Acta Crystallogr.* **1965**, *18*, 437−443.
(38) Hähner, G.; Marti, A.; Spencer, N. D.; Caseri, W. R. Orientation and electronic structure of methylene blue on mica: A near edge x-ray absorption fine structure spectroscopy study. *J. Chem. Phys.* **1996**, *104*, 7749−7757.

https://doi.org/10.1021/acsomega.1c00686
ACS Omega 2021, 6, 12105−12113